Preparation, Characterization, and Optical Properties of Gold, Silver, and Gold−Silver Alloy Nanoshells Having Silica Cores

Jun-Hyun Kim, William W. Bryan, and T. Randall Lee*

Department of Chemistry, University of Houston, 4800 Calhoun Road, Houston, Texas 77204-5003

Received May 28, 2008. Revised Manuscript Received July 29, 2008

This report describes the structural and optical properties of a series of spherical shell/core nanoparticles in which the shell is comprised of a thin layer of gold, silver, or gold−silver alloy, and the core is comprised of a monodispersed silica nanoparticle. The silica core particles were prepared using the Stöber method, functionalized with terminal amine groups, and then seeded with small gold nanoparticles (∼2 nm in diameter). The gold-seeded silica particles were coated with a layer of gold, silver, or gold−silver alloy via solution-phase reduction of an appropriate metal ion or mixture of metal ions. The size, morphology, and elemental composition of the composite nanoparticles were characterized by field emission scanning electron microscopy (FE-SEM), energy-dispersive X-ray spectroscopy (EDX), X-ray diffraction (XRD), Fourier transform infrared (FT-IR) spectroscopy, thermal gravimetric analysis (TGA), dynamic light scattering (DLS), and transmission electron microscopy (TEM). The optical properties of the nanoparticles were analyzed by UV−vis spectroscopy, which showed strong absorptions ranging from 400 nm into the near-IR region, where the position of the plasmon band reflected not only the thickness of the metal shell, but also the nature of the metal comprising the shell. Importantly, the results demonstrate a new strategy for tuning the position of the plasmon resonance without having to vary the core diameter or the shell thickness.

Introduction

Metal nanoshells grown on dielectric core particles are of great interest due to their tunable optical properties from the ultraviolet to the near-infrared regions of the electromagnetic spectrum.[1−5] These unique metal nanoparticles, whose optical properties differ from those of the corresponding solid metal nanospheres, represent one of the most useful of the recently developed nanoparticle structures prepared by wet-chemistry methods.[2,6] The most notable optical feature of metal nanoshells is the surface plasmon resonance, which arises from the collective oscillation of conducting electrons on the surface of the metal. Unlike simple metal nanoparticles, the surface plasmon of metal nanoshells can be tuned over a wide range of frequencies by varying the core size and shell thickness.[2] The structure and composition of these particles can also be adjusted in a controllable way to manipulate other physical properties (e.g., magnetic, mechanical, thermal, electrical, electro-optical, and catalytic).[7−12] Gold and silver metal nanoshells are of special interest to researchers not only because of their tunable optical properties,[13−15] but also because of their inertness in biological media.[16−18] These materials have substantial potential in a wide range of applications, including optical communications, laser-tissue welding, cancer therapy, and medical imaging.[19−22]

Gold shell-silica core particles have been successfully fabricated and used as band-pass optical filters, Raman enhancers, quenchers of conjugated polymer oxidation, and nanoscale platforms for drug-delivery.[3,9,23,24] Silica nanoparticles represent a convenient dielectric core, as they can be grown with a low polydispersity (less than 1%). Furthermore, methods for modifying the surface of silica with organic molecules are well developed.[25−27] These core particles can then be modified with small gold seeds, which allow for the preparation of gold, silver, and gold−silver alloy nanoshells via seed-mediated growth.[5,18,28,29] Nanoscale gold shells with strong optical absorbances provide a unique method for optical heating, as optical stimulation of the plasmon resonance causes the particles to become hot.[30,31] This heating can be

* To whom correspondence should be addressed. E-mail: trlee@uh.edu.

(1) Graf, C.; van Blaaderen, A. *Langmuir* **2002**, *18*, 524.
(2) Oldenburg, S. J.; Averitt, R. D.; Westcott, S. L.; Halas, N. J. *Chem. Phys. Lett.* **1998**, *288*, 243.
(3) Jackson, J. B.; Halas, N. J. *J. Phys. Chem. B* **2001**, *105*, 2743.
(4) Jain, P. K.; El-Sayed, M. A. *J. Phys. Chem. C* **2007**, *111*, 17451.
(5) Wang, H.; Tam, F.; Grady, N. K.; Halas, N. J *J. Phys. Chem. B.* **2005**, *109*, 18218.
(6) Oldenburg, S. J.; Jackson, J. B.; Westcott, S. L.; Halas, N. J. *Appl. Phys. Lett.* **1999**, *75*, 2897.
(7) Ji, X.; Shao, R.; Elliott, A. M.; Stafford, R. J.; Esparza-Coss, E.; Bankson, J. A.; Liang, G.; Luo, Z.; Park, K.; Markert, J. T.; Li, C. *J. Phys. Chem. C* **2007**, *111*, 6245.
(8) Mazurenko, D. A.; Shan, X.; Stiefelhagen, J. C. P.; Graf, C. M.; van Blaaderen, A.; Dijkhuis, J. I. *Phys. Rev. B* **2007**, *75*, 161102.
(9) Kim, J.-H.; Lee, T. R. *J. Biomed. Pharm. Eng.* **2008**, *2*, 29.
(10) Liao, Y.; Li, W.; He, S. *Nanotechnology* **2007**, *18*, 375701.
(11) Jian, Z.; Zhang, C. *J. Appl. Phys.* **2006**, *100*, 026104.
(12) Kim, J.-H.; Chung, H. W.; Lee, T. R. *Chem. Mater.* **2006**, *18*, 4115.
(13) Averitt, R. D.; Sarkar, D.; Halas, N. J. *Phys. Rev. Lett.* **1997**, *78*, 4217.
(14) Oldenburg, S. J.; Hale, G. D.; Jackson, J. B.; Halas, N. J. *App. Phys. Lett.* **1999**, *75*, 1063.
(15) Hu, M.; Chen, J.; Li, Z.; Au, L.; Hartland, G. V.; Li, X.; Marquez, M.; Xia, Y. *Chem. Soc. Rev.* **2006**, *35*, 1084.
(16) Shukla, R.; Bansal, V.; Chaudhary, M.; Basu, A.; Bhonde, R. R.; Sastry, M. *Langmuir* **2005**, *21*, 10644.
(17) Skrabalak, S. E.; Chen, J.; Au, L.; Lu, X.; Li, X.; Xia, Y. *Adv. Mater.* **2007**, *19*, 3177.
(18) Kim, J.; Park, S.; Lee, J. E.; Jin, S. M.; Lee, J. H.; Lee, I. S.; Yang, I.; Kim, J. S.; Kim, S. K.; Cho, M. H.; Hyeon, T. *Angew. Chem., Int. Ed.* **2006**, *45*, 7754.
(19) Wang, S. M.; Xiao, J. J.; Yu, K. W. *Opt. Commun.* **2007**, *279*, 384.
(20) Gobin, A. M.; O'Neal, D. P.; Watkins, D. M.; Halas, N. J.; Drezek, R. A.; West, J. L. *Las. Surg. Med.* **2005**, *37*, 123.
(21) Gobin, A. M.; Lee, M. H.; Halas, N. J.; James, W. D.; Drezek, R. A.; West, J. L. *Nano Lett.* **2007**, *7*, 1929.
(22) Wu, C.; Liang, X.; Jiang, H. *Opt. Commun.* **2005**, *253*, 214.
(23) Goude, Z. E.; Leung, P. T. *Solid State Commun.* **2007**, *143*, 416.
(24) Hale, G. D.; Jackson, J. B.; Shmakova, O. E.; Lee, T. R.; Halas, N. J. *Appl. Phys. Lett.* **2001**, *78*, 1502.
(25) Stöber, W.; Fink, A.; Bohn, E. *J. Colloid Interface Sci.* **1968**, *26*, 62.
(26) Van Helden, A. K.; Vrij, A. *J. Colloid Interface Sci.* **1980**, *78*, 312.
(27) Leite, C. A. P.; de Souza, E. F.; Galembeck, F. *J. Braz. Chem. Soc.* **2001**, *12*, 519.
(28) Jiang, Z.-j.; Liu, C.-y *J. Phys. Chem. B* **2003**, *107*, 12411.
(29) Pham, T.; Jackson, J. B.; Halas, N. J.; Lee, T. R. *Langmuir* **2002**, *18*, 4915.
(30) Neeves, A. E.; Birnboim, M. H. *J. Opt. Soc. Am. B: Opt. Phys.* **1989**, *6*, 787.
(31) O'Neal, D. P.; Hirsch, L. R.; Halas, N. J.; Payne, J. D.; West, J. L. *Cancer Lett.* **2004**, *109*, 171.

10.1021/la8016497 CCC: $40.75
Published on Web 09/13/2008

achieved in vivo with nanoshells tailored to absorb near-infrared light, since these wavelengths are not absorbed by skin or bone.[32,33]

Previously, researchers have modified the core sizes and/or shell thicknesses of monometallic nanoshells to give structures with tunable optical properties.[1,6] However, little attention has been given to the development of new types of nanoscale materials using bimetallics or trimetallics (e.g., alloys) that possess a multitude of properties that vary with their compositions.[34−40] In addition, these alloy materials can fulfill optical requirements that monometallics fail to achieve.[35,38,41] Here, we examine a system in which constant core and shell sizes but systematically varied shell materials give rise to particles with tunable optical properties. The fabrication method allows for the formation of gold, silver, and silver−gold alloy nanoshells with identical core sizes and shell thicknesses but distinct optical properties ranging from the visible to the near-infrared spectral regions. We anticipate that this type of red-shifting of the plasmon resonance to wavelengths in the visible and near-infrared regions of the spectrum—the so-called "water window"—will prove to be of tremendous importance for optically driven biomedical applications.[32,33]

Experimental Section

Materials. All reagents were purchased and used as received from the indicated suppliers: sodium hydroxide, formaldehyde, ammonium hydroxide (30% NH_3), trisodium citrate dihydrate, nitric acid, hydrochloric acid (all from EM Science), tetrakis(hydroxymethyl)phosphonium chloride (THPC, 80% in water), tetraethylorthosilicate (TEOS), 3-aminopropyltrimethoxysilane (APTMS; all from Aldrich), potassium carbonate (J. T. Baker), ethanol (McKormick Distilling Co.), silver nitrate (Mallinckrodt), and hydrogen tetrachloroaurate(III) hydrate (Strem). Deionized water was purified to a resistance of 18 MΩ (Milli-Q Reagent Water System; Millipore Corporation) and filtered using 0.2 μm membrane filter to remove any impurities. All glassware and equipment were first cleaned in an aqua regia solution (3:1, HCl/HNO_3), followed by soaking extensively in a base bath (saturated KOH in isopropyl alcohol), and finally rinsed with Milli-Q water prior to use.

Preparation of Amine-Functionalized Silica Nanoparticles. This procedure represents a slight modification of the well-known Stöber method to prepare large silica core particles.[25] Ammonium hydroxide (NH_4OH, 26.8 mL) was added to 200 mL of absolute ethanol in a 500 mL two-necked round-bottomed flask and stirred at 30 °C for 30 min. An aliquot of tetraethylorthosilicate (TEOS, 6 mL) was quickly added to the mixture, which was stirred overnight to afford monodisperse silica nanoparticles. Excess aminopropyltrimethoxysilane (APTMS, 0.5 mL) was then added to the silica particle solution. The solution was vigorously stirred for 6−8 h and refluxed for 1 h to promote covalent bonding of the APTMS moieties to the surface of the silica particles.[42,43] The amine-functionalized silica particles were centrifuged (RC-3B Refrigerated Centrifuge from Sorvall Instruments) at 2500 rpm for 1 h and redispersed twice in 200 mL of ethanol. While analysis by FE-SEM and TEM showed no substantial differences between unfunctionalized and APTMS-functionalized silica particles, FT-IR and TGA measurements confirmed the attachment of APTMS on silica nanoparticles (see Figure S1 in the Supporting Information).

THPC Gold Seed Preparation and Attachment to Amine-Functionalized Silica Nanoparticles. A solution of small gold seeds was prepared by reduction of hydrogen tetrachloroaurate(III) hydrate with tetrakis(hydroxymethyl)phosphonium chloride (THPC) using a modification of the method reported by Duff et al.[44−46] An aliquot of sodium hydroxide solution (1.0 mL, 0.024 g, 0.6 mmol), 2 mL of THPC solution (12 μL of THPC in 1 mL of water), and 200 mL of Milli-Q water were mixed in a 250 mL flask and vigorously stirred for at least 15 min. An aliquot (4 mL) of 1 wt % aqueous $HAuCl_4 \cdot H_2O$ was quickly added to the mixture. The color of the solution changed rapidly from colorless to dark reddish yellow. Stirring was continued for ~30 min. The solution was then stored in the refrigerator for at least three days before use. The resultant gold nanoparticle seeds were consistently observed to be ~2−3 nm in diameter.

We attached the gold seeds to the silica core nanoparticles using a modification of the Westscott et al. method described in detail elsewhere.[47] Briefly, the THPC gold seeds were deposited onto the silica particles by mixing aged THPC gold seeds, which were concentrated from 50 mL to ~10 mL by rotary evaporation, and 1 mL of amine-functionalized silica nanoparticles overnight. The final solution was light red in color after the precipitate was redispersed in water.

K-Gold, K-Silver, and K-Alloy Preparation. A potassium-containing basic solution of gold salt (K-gold solution) was prepared by adding 0.05 g of potassium carbonate (K_2CO_3) to 200 mL of water, stirring for 15 min to dissolve the K_2CO_3 completely, and adding 4 mL of 1 wt % $HAuCl_4 \cdot H_2O$ solution. The color of the mixture changed from yellow to colorless within 40 min. We prepared K-silver solutions (using 2 mL of 1 wt % $AgNO_3$) and K-alloy solutions (using 1 mL of 1 wt % $AgNO_3$ + 2 mL of 1 wt % $HAuCl_4 \cdot H_2O$) using analogous procedures.

Gold, Silver, and Gold−Silver Alloy Nanoshell Growth.[2] To grow the gold−silver alloy layer on the THPC gold attached silica nanoparticles, 8 mL of the prepared K-alloy solution was placed in a 25 mL beaker containing a magnetic stirring bar. Varying amounts of THPC gold-seeded silica nanoparticle solution (0.5−2 mL) were then added to produce different thicknesses of gold−silver alloy nanoshells. After stirring the mixture for 10 min, 0.02 mL of formaldehyde and 0.05 mL of ammonium hydroxide were added simultaneously to reduce the K-alloy solution. The color of solution changed from colorless to dark blue, dark green, and green depending on the shell thickness. The alloy nanoshells were centrifuged and redispersed in Milli-Q water to remove any unreacted chemicals and small seed particles. Silver nanoshells were prepared in the same manner, as were gold nanoshells, but the latter used no ammonium hydroxide. For silver and gold nanoshells, the color changes varied similar to those described above depending on the shell thickness as well as the relative content of gold and silver.

Characterization Methods. To demonstrate the overall uniformity and morphology of the particles, the samples were examined by field emission scanning electron microscopy (FE-SEM) using a JSM 6330F JEOL instrument operating at 15 kV. For high-resolution images, all samples were placed on a carbon-coated copper grid and dried at room temperature overnight. To enhance the electrical conductivity, the samples were coated with carbon via sputtering. Higher resolution images were obtained by transmission electron microscopy (TEM) using a JEM-2000 FX JEOL instrument at an accelerating voltage of 200 kV

(32) Simpson, C. R.; Kohl, M.; Essenpreis, M.; Cope, M. *Phys. Med. Biol.* **1998**, *43*, 2465.
(33) Gorelikov, I.; Field, L. M.; Kumacheva, E. *J. Am. Chem. Soc.* **2004**, *126*, 15938.
(34) Liu, J.-H.; Wang, A.-Q.; Chi, Y.-S.; Lin, H.-P.; Mou, C.-Y. *J. Phys. Chem. B* **2005**, *109*, 40.
(35) Zhang, J.; Liu, H.; Wang, Z.; Ming, N. *J. Solid State Chem.* **2007**, *180*, 1291.
(36) Link, S.; Wang, Z. L.; El-Sayed, M. A. *J. Phys. Chem. B* **1999**, *103*, 3529.
(37) Liu, J. B.; Dong, W.; Zhan, P.; Wang, S. Z.; Zhang, J. H.; Wang, Z. L. *Langmuir* **2005**, *21*, 1683.
(38) Seo, D.; Yoo, C. I.; Jung, J.; Song, H. *J. Am. Chem. Soc.* **2008**, *130*, 2940.
(39) Radziuk, D.; Shchukin, D.; Mohwald, H. *J. Phys. Chem. C* **2008**, *112*, 2462.
(40) Sato, T.; Kuroda, S.; Takami, A.; Yonezawa, Y.; Hada, H. *Appl. Organomet. Chem.* **1991**, *5*, 261.
(41) Peng, Z.; Spliethoff, B.; Tesche, B.; Walther, T.; Kleinermanns, K *J. Phys. Chem. B* **2006**, *110*, 2549.
(42) Waddell, T. G.; Leyden, D. E.; DeBello, M. T. *J. Am. Chem. Soc.* **1981**, *103*, 5303.
(43) van Blaaderen, A.; Vrij, A. J. *J. Colloid Interface Sci.* **1993**, *156*, 1.
(44) Duff, D. G.; Baiker, A. *Langmuir* **1993**, *9*, 2301.
(45) Duff, D. G.; Baiker, A. *Langmuir* **1993**, *9*, 2310.
(46) Teo, B. K.; Keating, K.; Kao, Y.-H. *J. Am. Chem. Soc.* **1987**, *109*, 3494.
(47) Westscott, S. L.; Oldenburg, S. J.; Lee, T. R.; Halas, N. J. *Langmuir* **1998**, *14*, 5396.

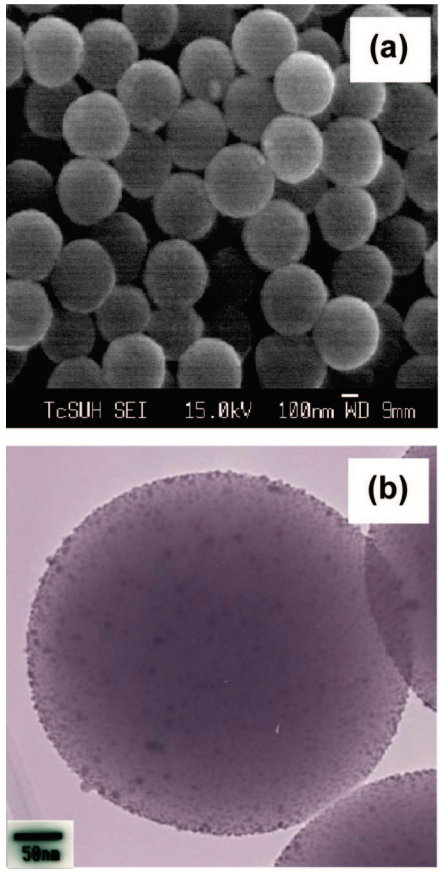

Figure 1. THPC gold seeds on silica core particles: (a) FE-SEM and (b) TEM images.

and equipped with an energy dispersive X-ray spectroscopy (EDX) analyzer (Link analytical EXL, Oxford). All TEM samples were deposited on 300 mesh Holey carbon-coated copper grids and dried overnight before examination. UV−vis spectra were obtained using a Cary 50 Scan UV−vis spectrometer over the wavelength range of 300−1100 nm. All samples were centrifuged and redispersed in Milli-Q water prior to analysis. For dynamic light scattering (DLS) measurements, an ALV-5000 Multiple Tau Digital Correlation instrument operating at a light source wavelength of 514.5 nm and a fixed scattering angle of 90° was used to measure the average hydrodynamic diameters for all nanoshell particles. To confirm the formation of gold−silver alloy nanoshells, powder X-ray diffraction (PXRD) patterns were recorded with a Rigaku XDS 2000 diffractometer using nickel-filtered Cu Kα radiation (λ = 1.5418 Å).

Results and Discussion

Figure 1 shows typical FE-SEM and TEM images of silica nanoparticles decorated with THPC gold seeds. While the FE-SEM images are insufficiently resolved to detect the THPC gold seeds, the TEM images clearly show 2−3 nm THPC gold seeds attached to the surfaces of the silica nanoparticles. These data are consistent with the results of previous work showing mostly isolated and a few partially aggregated gold seeds attached to APTMS-modified silica surfaces.[47] Based on several FE-SEM and TEM images, the average diameter of the seeded silica core particles studied here is ∼430 nm, which is consistent with analysis by DLS (data not shown).

Figure 2 shows the extinction spectra of the free THPC gold seeds and gold seeds deposited on the silica core particles. The aged THPC gold seeds show a weak plasmon band at 510 nm, which is consistent with that known for small (≤10 nm) gold nanoparticles.[44] Gold seeds having these sizes exhibit no striking

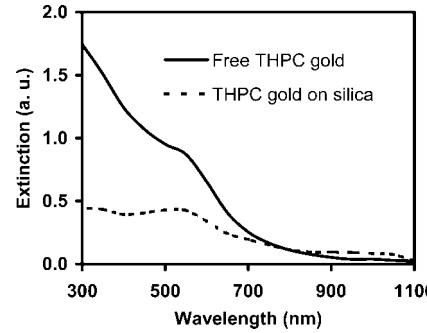

Figure 2. UV−vis spectra of free gold seeds and gold seeds attached to silica core particles.

plasmon band compared to that of larger gold nanoparticles (i.e., >20 nm), which exhibit an intense absorption at ∼550 nm.[48] Upon attachment to silica nanoparticles, the plasmon band THPC gold seeds appears at ∼520 nm, which is slightly red-shifted compared to that of the free gold seeds. The red-shift of the plasmon band is due to the partial colloidal aggregation of the gold seeds on the surface of the silica particles. The presence of gold seeds on silica particles also supports the attachment of APTMS on the silica surface analyzed by FT-IR and TGA (see Figure S1 in the Supporting Information).

To coat the silica particles with gold, silver, or gold−silver alloy in water, a seeded-growth method was used in which THPC seed nanoparticles act as nucleation sites.[49] The reduction of added gold and/or silver ions reproducibly leads to coalescence into complete metal nanoshells. Nanoshell growth is complete within a few seconds upon the addition of K-gold and/or K-silver solution and both formaldehyde and ammonium hydroxide. From the FE-SEM and TEM images (typical examples are shown in Figure 3), we can estimate the general size distribution of the nanoshell particles. Given that the silica core diameters are ∼430 nm, we infer that the gold, silver, and alloy shells are ∼15 nm thick. The micrographs show that all of the nanoshells are spherical, but their surface is somewhat rough, particularly for the silver and alloy nanoshells.

We were able to increase systematically the thickness of the shells by decreasing the amounts of THPC-gold seeded silica core particles added to the K-metal solution. Figure 4 shows the formation of gold, silver, and alloy nanoshells with enhanced shell thickness (∼30 nm). The TEM images show that the gold nanoshell surfaces are smoother than the surfaces of the other two metal nanoshells, which is consistent with observations of the thinner shells (Figure 3). Regarding the thicker nanoshells, this difference can also be observed in the lower resolution FE-SEM images as well as low magnification TEM images (see Figure S2 in the Supporting Information). Others have reported similar difficulties in efforts to fabricate silver nanoshells with smooth surfaces.[28,50−52] Our experiences here and in separate studies involving the synthesis of simple monometallic nanoparticles suggests that silver is less amenable than gold to form nanoparticles with smooth surface morphologies. Nevertheless, when taken as a whole, the images in Figures 3 and 4 demonstrate

(48) Turkevich, J.; Stevenson, P. C.; Hillier, J. *Discuss. Faraday Soc.* **1951**, *58*, 55.
(49) Radloff, C; Vaia, R. A.; Brunton, J.; Bouwer, G. T.; Ward, V. K. *Nano Lett.* **2005**, *5*, 1187.
(50) Yong, K.-T.; Sahoo, Y.; Swihart, M. T.; Prasad, P. N. *Colloids Surf., A* **2006**, *290*, 89.
(51) Mayer, A. B. R.; Grebner, W.; Wannemacher, R. *J. Phys. Chem. B* **2000**, *104*, 7278.
(52) Peterson, M. S. M.; Bouwman, J.; Chen, A.; Deutsch, M. *J. Colloid Interface Sci.* **2007**, *306*, 41.

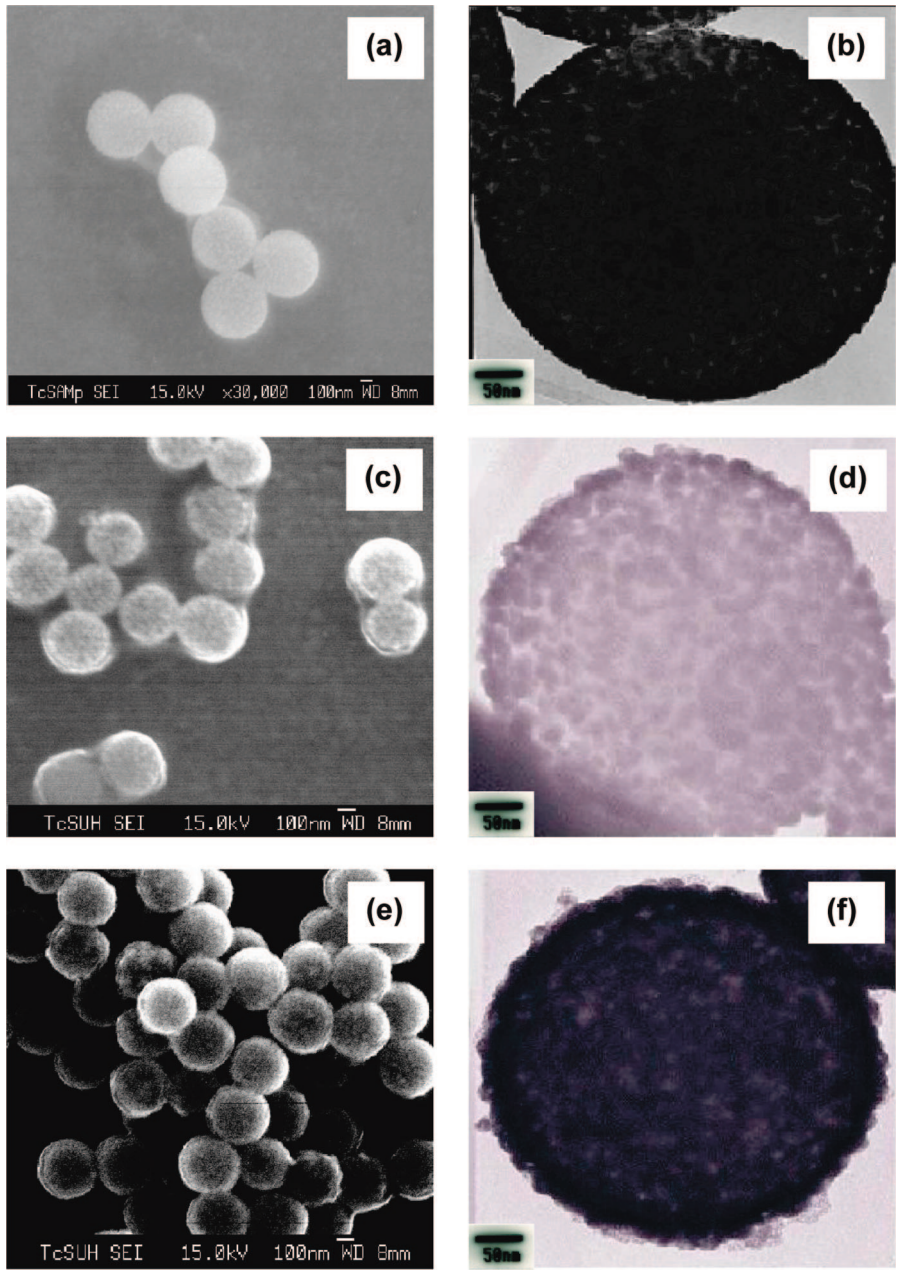

Figure 3. FE-SEM images of (a) gold, (c) silver, and (e) alloy shells; TEM images of (b) gold, (d) silver, and (f) alloy shells. Dimensions: ~430 nm silica cores with ~15 nm shell thicknesses.

that the seeded-growth method allows for the preparation of gold, silver, and gold−silver alloy nanoshells in a reproducible fashion, having controllable thicknesses at the nanometer scale (see Figure S3 in the Supporting Information). We also note that under similar reaction conditions (concentrations of core nanoparticles and K-metal growth solution), thick nanoshells with rough surface morphologies were formed as the amount of silver content increased (see Figure S4 in the Supporting Information).

To confirm the formation of the gold−silver alloy nanoshells on the silica core nanoparticles, we collected EDX spectra over random areas to monitor the elemental composition. The EDX spectrum in Figure 5 shows characteristic peaks for gold (Mα and Lα at 2.12 and 9.71 keV, respectively) and silver (Lα and Lβ at 2.95 and 3.15 keV, respectively). A small copper peak is also present due to X-ray emission from the supporting copper grid. The presence of gold and silver peaks is consistent with the formation of alloy shells on the silica cores. The intensities of the gold peaks are slightly stronger than those of silver collected at the same energy level because of the slightly higher composition of gold from the starting material composed of THPC gold seeds on silica nanoparticles (see the Experimental Section). EDX analyses also indicate a slightly higher intensity for gold than for silver, which is consistent with quantitative analysis of compositions (see Table S1 in the Supporting Information). The EDX analyses of the Au−Ag alloy shells closely resemble the starting metal compositions (THPC gold seeds do not significantly affect the final composition of alloys). Thus, EDX analysis provides further evidence for the formation of alloy nanoshells using different ratios of silver and gold solutions (e.g., mole fraction: Ag 100%, Ag 75%, Ag 50%, Ag 25%, and Ag 0%). The corresponding alloy nanoshells are shown in Figure S4 in the Supporting Information.

To verify the formation of alloy nanoparticles, we employed X-ray diffraction (XRD) and measured the powder patterns of pure gold, silver, and gold−silver alloy nanoshells (1:1) on silica core nanoparticles. All of the monometallic and bimetallic samples

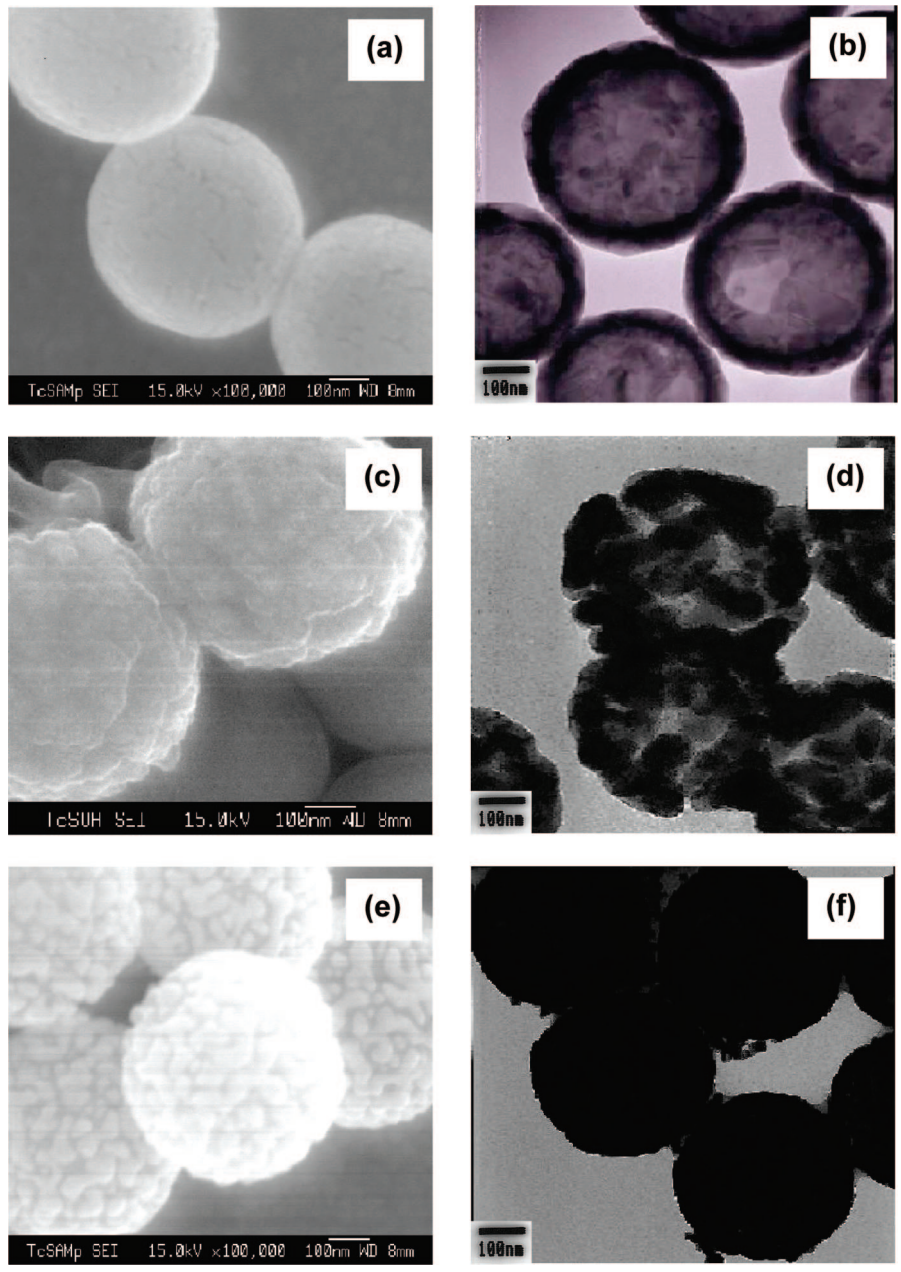

Figure 4. FE-SEM images of (a) gold, (c) silver, and (e) alloy shells; TEM images of (b) gold, (d) silver, and (f) alloy shells. Dimensions: ~430 nm silica cores with ~30 nm shell thicknesses.

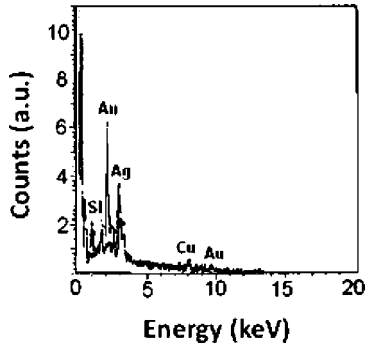

Figure 5. EDX spectrum of gold−silver alloy nanoshells (~30 nm shell thickness).

have similar XRD patterns, characterized by three peaks positioned at 2θ values of 38.2°, 44.4°, and 64.7°, which correspond to the (111), (200), and (220) lattice planes, respectively (see Figure S5 in the Supporting Information). Due to gold and silver having similar lattice constants (0.408 nm versus 0.409 nm),[53,54] the XRD pattern (or electron diffraction using TEM) was unable to provide definitive evidence for the formation of metal alloy nanoshells. However, the XRD pattern of the alloy nanoshells is consistent with the XRD patterns of the silver and gold nanoshells.

To provide further support for the formation of gold−silver alloys under our reaction conditions, we prepared gold−silver alloy nanoparticles in the absence of gold-seeded silica nanoparticles using K-alloy solution. The consequent observation of a single absorption centered at ~495 nm, where neither gold nor silver nanoparticles absorb, confirms the formation of alloy nanoparticles from the K-alloy solution (see Figure S6 in the Supporting Information). If a mixture of gold and silver nanoparticles were formed under our reaction conditions, one

(53) De, G.; Pal, S. *Chem. Mater.* **2005**, *17*, 6161.
(54) Kondarides, D. I.; Verykios, X. E. *J. Catal.* **1996**, *158*, 363.

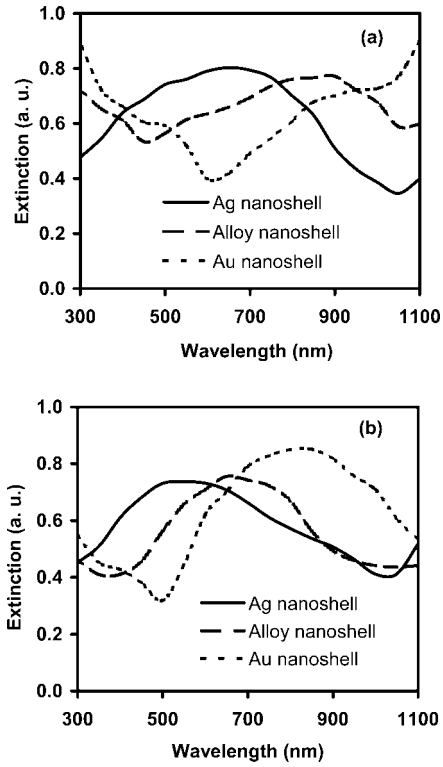

Figure 6. UV−vis spectra of gold, silver, and gold−silver alloy nanoshells having ~430 nm silica cores with (a) ~15 nm shell thickness and (b) ~30 nm shell thickness.

would have observed instead two distinctive absorption peaks at 420 nm for silver and 530 nm for gold nanoparticles, respectively.[36]

Figure 6a shows the UV−vis spectra of the thinner gold, silver, and gold−silver alloy shells (~15 nm thickness) on the silica core particles (~430 nm in diameter). At a constant shell thickness, the UV−vis spectra show broad absorption bands from the visible to the near-infrared depending on the shell materials (i.e., gold, silver, gold−silver alloy). Silver nanoshells exhibit the shortest absorption wavelengths (500−750 nm), but these wavelengths are still substantially longer than those observed for simple silver nanoparticles (~420 nm).[36] Meanwhile, gold nanoshells exhibit the longest absorption wavelength (>800 nm). It is known that the absorption wavelength of simple gold nanoparticles (~530 nm) is ~150 nm higher than that of simple silver nanoparticles.[55] For nanoshells, the absorption wavelength of gold nanoshells is again higher than that of silver nanoshells, but the difference is amplified. Additionally, different shell thicknesses of gold−silver alloy nanoshells on silica nanoparticles were prepared, giving rise to tunable absorption bands from visible to near IR spectral regions (see Figure S7 in the Supporting Information). As a whole, the absorption spectra of metal nanoshells on silica core nanoparticles can be systematically tuned either by the shell materials or shell thicknesses.

Simple gold−silver alloy nanoparticles are known to have an absorption wavelength that falls in between those of simple gold and silver nanoparticles; the exact band position depends on the ratio of each metal.[36] Figure 6a shows that gold−silver alloy nanoshells show the same trend, but the band positions of the nanoshells are red-shifted and broadened relative to those of the corresponding simple alloy nanoparticles.[36] The position, intensity, and broadening of the absorption bands can be understood qualitatively on the basis of Mie theory.[56,57] Moreover, the position of the bands arising from dipole, quadrupole, and higher order resonances is influenced by the shell materials (i.e., gold, silver, gold−silver alloy). It is also known that the absorption intensity of metal nanoshell particles increases when the shell growth is complete.[1] The intense absorptions observed here suggest complete coverage of the silica surfaces; this conclusion is consistent with the microscopy images shown in Figures 3 and 4, as well as the EDX data (e.g., Figure 5). As described previously,[6,14,58] it is likely that the peak broadening of the spectra in Figure 6a arises in part from (1) the polydispersity of the core particles, (2) the roughness of the shell surfaces, (3) the presence of a few particles with incomplete shells, and/or (4) the overlap of multipole surface plasmon resonances (e.g., quadrupole and octupole) arising from the large nanoshell particles. The latter is perhaps important here since the particles are approaching microscale dimensions.

Figure 6b shows the optical properties of the thicker metal shells (~30 nm) grown on the silica core particles. Compared to Figure 6a, we find that all of the nanoshells absorb at shorter respective wavelengths due to the increase in the thickness of the shell,[1,2,49] but the relative order of the absorption maxima remains unchanged (i.e., gold > alloy > silver). We note further that the spectra are consistent with the work of Graf and van Blaaderen,[1] where the position of the absorption band is expected to become decreasingly affected by increasing the thickness of the shell (~30 nm), but the general shape of the absorption band is likely to change with increasing shell thickness. Taken as a whole, the spectra in Figure 6 demonstrate an alternative "alloying" strategy for tuning the position of the plasmon resonance of metal nanoshells.

Conclusions

We report a reliable synthesis method that leads to the formation of gold−silver alloy nanoshells on dielectric silica core particles. This method enables one to tune the absorption wavelength of metal nanoparticles from the visible to the near-IR regions simply by changing the composition of the shell rather than altering core sizes and/or shell thicknesses. The preparation of these particles and their incorporation into various supporting media should give rise to devices that can be optically modulated across wavelengths where few competing materials currently exist. In particular, these new alloy nanoshells should find use in applications involving cancer screening, optical switching, and surface-enhanced Raman Scattering (SERS).

Acknowledgment. We thank the Army Research Office, the Texas Center for Superconductivity, and the Robert A. Welch Foundation (Grant No. E-1320) for financial support. We also thank Dr. J. K. Meen for assistance with the FE-SEM measurements and Dr. I. Rusakova for assistance with the TEM measurements.

Supporting Information Available: TGA, FT-IR, XRD, UV−vis, and EDX, as well as low magnification TEM and SEM images, are provided to clarify gold−silver alloy formations. This material is available free of charge via the Internet at http://pubs.acs.org.

LA8016497

(55) Heard, S. M.; Grieser, F.; Barraclough, C. G.; Sanders, J. V. *J. Colloid Interface Sci.* **1983**, *93*, 545.
(56) Mie, G. *Ann. Phys.* **1908**, *25*, 377.
(57) Aden, A. L.; Kerker, M. *J. Appl. Phys.* **1951**, *22*, 1242.
(58) Oldenburg, S. J.; Westcott, S. L.; Averitt, R. D.; Halas, N. J. *J. Chem. Phys.* **1999**, *111*, 4729.